# Molecular characteristics of permanganate and dichromate oxidation resistant soil organic matter from a Black C rich colluvial soil

Manuel Suárez-Abelenda[a*], Joeri Kaal[b], Marta Camps-Arbestain[c], Heike Knicker[d], Felipe Macías[a]

[a] Departamento de Edafoloxía e Química Agrícola, Facultade de Bioloxía, Universidade de Santiago de Compostela, 15782- Santiago de Compostela, Spain

[b] Instituto de Ciencias del Patrimonio (Incipit), Consejo Superior de Investigaciones Científicas (CSIC), Rúa San Roque 2, 15704 Santiago de Compostela, Spain.

[c] Institute of Natural Resources, Private Bag 11222, Massey University, Palmerston North 4442, New Zealand.

[d] Instituto de Recursos Naturales y Agrobiología de Sevilla (IRNAS-CSIC), Adva. Reina Mercedes, 10, 41012 Sevilla, Spain.

* Corresponding author (M. Suárez Abelenda): Departamento de Edafoloxía e Química Agrícola, Facultade de Bioloxía, Universidade de Santiago de Compostela, 15782- Santiago de Compostela, Spain. Tel.: +34 881816039. E-mail address: manuel.suarez@usc.es.

**Abstract**

Samples from a colluvial soil rich in pyrogenic material (Black C, BC) in NW Spain were subjected to $K_2Cr_2O_7$ and $KMnO_4$ oxidation and the residual soil organic matter (SOM) was NaOH-extracted and analyzed using analytical pyrolysis–gas chromatography–mass spectroscopy (Py-GC/MS) and solid-state $^{13}C$ cross polarization–magic angle spinning–nuclear magnetic resonance ($^{13}C$ CP MAS-NMR) in order to study the susceptibility of different SOM fractions (fresh, degraded/microbial, BC and aliphatic) towards these oxidizing agents. NaOH extracts of untreated samples were also analyzed. Py-GC/MS and $^{13}C$ NMR indicated that $KMnO_4$ promotes the oxidation of carbohydrate products, mostly from degraded/microbial SOM and lignocellulose, causing a relative enrichment of aliphatic and aromatic structures. Residual SOM after $K_2Cr_2O_7$ oxidation contained BC, N-containing BC and aliphatic structures. This was corroborated by a relatively intense resonance of aromatic C and some signal of alkyl C in $^{13}C$ NMR spectra. These results confirm that dichromate oxidation residues contain a non-pyrogenic fraction mainly consisting of aliphatic structures.

## 1. Introduction

Soil organic matter (SOM) is a complex mixture of plant, animal and microbial tissue, both fresh and at different stages of decomposition (Stevenson 1994; Tabatabai 1996). The molecular structures present in SOM have been a source of debate for many decades due the analytical difficulties inherent to SOM characterization (Piccolo 1996). A wide set of methodologies have been used to study SOM composition, including 1) fractionation methods such as (i) chemolytic techniques (i.e. application of acid-hydrolysis or extracting agents) that are coupled with colorimetric and/or GC/MS analyses to identify specific SOM components (polysaccharides, lignin-derived compounds, amino sugars, extractable- lipids or hydrolysable proteins) (Kögel-Knabner 1995); (ii) physical fractionation into organo- mineral fractions based on particle size and/or density yields (Christensen 1992; Six et al. 2002); (iii) wet oxidation with potassium permanganate ($KMnO_4$) (Loginow et al. 1987; Tirol-Padre and Ladha 2004), $H_2O_2$ (Eusterhues et al. 2005), $Na_2S_2O_8$ (Eusterhues et al. 2003), NaOCl (Kleber et al. 2005), and $K_2Cr_20_7$ (Skjemstad and Taylor 1999); and 2) analytical techniques including (i) spectroscopic techniques, such as infrared (IR) spectroscopy and solid-state $^{13}C$ nuclear magnetic resonance ($^{13}C$ NMR) (Wilson et al. 1981; Fründ et al. 1993) and (ii) pyrolysis-GC/MS (Py-GC/MS) (Sáiz-Jiménez and the Leeuw 1994a). Whereas IR and $^{13}C$ NMR provide information on the environment of carbon atoms (functional groups) (Baldock and Smernik 2002), more detail on the molecular chemistry is obtained by pyrolysis-GC/MS.

Py-GC/MS is based on thermal degradation in an inert atmosphere (pyrolysis) and subsequent separation (GC) and identification (MS) of the pyrolyzate, from which information on macromolecular structures can be extracted (Moldoveanu 1998). For example, it allows the identification of different sources and degradation states of plant

detritus, secondary/microbial material, Black C (BC), and the estimation of their relative proportions (Nierop et al. 2005; Buurman et al. 2007). Nonetheless, Py-GC/MS is a semi-quantitative method because of differences in the pyrolyzability of different organic matter components, not all pyrolysis products are amenable and detectable by GC, and differences in relative response factors by MS (Sáiz-Jiménez 1994a)

The Walkley-Black dichromate oxidation, as modified by Heanes (1984), is a relatively simple and rapid procedure with minimal equipment needs (Nelson and Sommers 1996) that has long been used to estimate the organic C (OC) content of soils. Its major disadvantage is that it incompletely oxidizes soil OC (Gillman et al. 1986), and has different oxidation efficiencies for different soils (Tabatabai 1996), which produce considerable and unpredictable deviations from 'true' soil OC content. Probable causes of deviations in recoveries are (i) spatial inaccessibility of organic substrates to the oxidation agent (Skjemstad et al. 1996; Six et al. 2002), (ii) binding with inorganic phases (Eusterhues et al. 2005) and (iii) the presence of chemically recalcitrant SOM fractions such as BC (Six et al. 2002). In fact, the difference between total OC and dichromate-oxidizable OC has been used to estimate the BC content of soils. BC is defined as the product resulting from incomplete thermal combustion of vegetation and/or fossil fuels, and is relatively resistant to decomposition (Schmidt et al. 2001). However, an unknown portion of BC is actually oxidized while some non-pyrogenic SOM may survive the oxidation, e.g. non-hydrolyzable aliphatic compounds that resist aqueous dichromate oxidation (Knicker et al. 2007). This implies that the properties of the oxidation-resistant residue must be assessed in order to obtain meaningful estimations of BC content using dichromate oxidation (Knicker et al. 2007). The stability of BC towards these reagents is of significant interest considering its upcoming use as a soil amendment (as biochar).

The permanganate-oxidizable fraction has been used as a proxy for the labile fraction of SOM (Loginow et al. 1987, Lefroy et al. 1993), based on the assumption that the oxidative capacity of $KMnO_4$ on SOM is comparable to that of soil microbial enzymes (Conteh et al. 1997). However, some studies indicated that $KMnO_4$- oxidizable C may not be a reliable measure of the proportion of labile C because, even though it efficiently degrades lignin (van Soest and Wine 1986), it has little effect on several SOM components that are widely recognised as easily degraded by soil microorganisms, e.g. structural carbohydrates, sugars and amino acids (e.g. Tyrol-Padre and Ladha 2004). Furthermore, its ability to react with charcoal was also stated (Skjemstad et al. 2006).

SOM is thermodynamically unstable in well-aerated soils (Macías and Camps-Arbestain 2010). However, SOM stabilized by specific mechanisms can remain as meta-stable forms in soils for hundreds to thousands of years (Six et al. 2002). These non-ideal conditions for SOM decay are associated to physical and chemical protection mechanisms offered by the soil matrix that either impede the access of enzymes to SOM (e.g., within microaggregates or by creating hydrophobicity) or increase the energy needed to degrade SOM through interactions with minerals (Eusterhues et al. 2003). In addition, enhanced SOM preservation may occur when environmental conditions are not adequate for microbial growth, e.g. the presence of free Al and Fe, low soil pH and/or due to low nutrient availability (Buurman and Roscoe 2011). Furthermore, intrinsic recalcitrance of specific SOM components may increase its longevity in soil. This is most likely the main process responsible for the long turn-over time of highly condensed aromatic compounds present in BC (Harvey et al. 2012).

The nature of permanganate- and dichromate-oxidation resistant SOM is still poorly understood. Here we study the molecular properties of $KMnO_4$- and $K_2Cr_2O_7$-

oxidation-resistant SOM from a BC-rich colluvial soil, by Py-GC/MS and solid-state $^{13}C$ NMR, which may add to our knowledge on the stability of specific organic compounds against soil microbial oxidative enzymes.

## 2. Material and methods

### *2.1. Study site and sample descriptions*

Soil PRD-4 is a 2.4 m thick Haplic Umbrisol (humic/alumic) according to the IUSS Working Group (2006) and Humic Pachic Dystrudept according to the SSS (1998). This soil type is traditionally referred to as Atlantic Ranker (Carballas et al. 1967). Radiocarbon dating showed that the soil gradually accumulated through colluviation during the last ca. 13,000 yr (Kaal et al. 2011). Soil PRD-4 has a deep black color owing to a combination of high SOM content and abundance of BC (Table 1). For the present study, three samples were selected from this soil, corresponding to three periods with radically different ecosystems and hypothetically also different SOM compositions: S1 (5-10 cm depth) corresponds to recent material (<150 y BP), evidenced by $^{14}C$ dating and the presence of pollen of exotic species *Eucalyptus* sp. (López-Merino et al. 2012) (Table 1). This soil layer contains considerable amounts of "fresh" (non- or slightly degraded) SOM and root fragments, as described by Kaal and van Mourik (2008). The vegetation corresponding to this sample is a mosaic of shrubland (dominated by Ericaceae), pasture and exotic tree species. Sample S2 (95-100 cm depth) contains large amounts of charcoal from palaeofires (Kaal et al. 2011) that occurred ca. 5,000 yr ago. Anthracological analysis showed that most charcoal originates from deciduous *Quercus* sp. This sample is thought to correspond to an oak-dominated woodland under substantial fire and grazing pressure. Sample S3 (190- 195 cm depth) corresponds to an Early- Holocene phase (ca. 9,700 yr BP) that preceded the

136 colonization of the area by deciduous forest, with "steppe-like" vegetation dominated
137 by *Betula* sp. (birch), shrubs of the Fabaceae family and herbaceous species.
138
139 *2.2. Determination of organic C fractions*
140 Potassium dichromate-oxidizable organic C ($OC_{dichro}$) was determined following
141 the Walkley-Black oxidation method as modified by Wolbach and Anders (1989) and
142 Knicker et al. (2007). 0.5 g of dry soil (< 2 mm) were oxidized in triplicate with 20 ml
143 of 0.2 M $K_2Cr_2O_7$ and 20 ml of concentrated $H_2SO_4$ at 60 °C in a water bath for 6 h.
144 Control samples without soil were also analyzed. After the reaction, excess dichromate
145 was determined by titration against 0.033 M $FeSO_4$. The amount of dichromate
146 consumed by the soil was used to calculate the amount of dichromate-oxidizable
147 organic C ($OC_{dichro}$) assuming that (i) the oxidation state of soil OC is zero ($C^0$) and (ii)
148 complete oxidation to $C^{+4}$ occurs.

149 Potassium permanganate-oxidizable organic C ($OC_{per}$) was determined, in
150 triplicate, using 25 ml of 33 mM $KMnO_4$ solution added in 50 ml centrifuge tubes
151 containing an amount of dry soil (<2 mm) equivalent to 15 mg organic C (Tirol-Padre
152 and Ladha 2004). After 24 h shaking, the tubes were centrifuged for 5 min at 2600 *g*
153 and the supernatant diluted in distilled water (1:25 v:v). Absorbance was read on a split
154 beam spectrophotometer at 565 nm. Blanks and a standard soil were analyzed before
155 each run. For calculation purposes, it was assumed that three moles of C (e.g.
156 carbohydrates) are oxidized for every four moles of $Mn^{+7}$ reduced (Tirol-Padre and
157 Ladha 2004).
158
159 *2.3. Isolation of SOM fractions*

The non-oxidized (NO) SOM extraction was considered the control treatment, consisting of SOM extraction by NaOH as described by Buurman et al. (2007). Briefly, 5 g soil (air- dried fine earth <2 mm) was extracted with 50 ml of 1 M NaOH and shaken for 24 h under $N_2$ to prevent oxidation/saponification. The suspension was centrifuged at 2600 *g* for 1 h and the extract decanted, after which the extraction was repeated. The two extracts were combined and the residues discarded. The extracts were then acidified to pH 1 with concentrated HCl to protonate SOM. One ml of concentrated HF was added to dissolve silicates and increase C content of the extracted fraction. The acid mixture was shaken for 48 h, after which it was dialyzed to neutral pH against distilled water to remove excess salt. Finally, the suspension was freeze- dried.

Dichromate oxidation-resistant SOM (CR): 12.5 g soil was oxidized in 500 ml of 0.2 M $K_2Cr_2O_7$ and 100 ml of concentrated $H_2SO_4$ for 6 h at 60 °C using a water bath. Once cooled, the suspension was centrifuged at 2600 *g* for 1 h and the supernatant decanted, after which the sediment was washed with distilled water until the solution was colorless. The suspension was discarded and the dichromate oxidation-resistant SOM extracted by 200 ml of 1 M NaOH for 24 h under $N_2$. The resultant suspension was centrifuged at 2600 g for 1 h and the supernatant decanted. This extraction was repeated twice. Thereafter, the three extracts were combined and acidified to pH 1 with concentrated HCl. One ml of concentrated HF was added to dissolve silicates and increase the content of organic C of the extracted fraction. This acid mixture was shaken for 48 h, dialyzed against $H_2O$ to neutral pH and finally freeze- dried.

Permanganate oxidation-resistant SOM (MN): 1000 ml of 33 mM $KMnO_4$ were added to 4.8, 8.2 and 7.0 g dry soil (<2 mm) for samples S1, S2 and S3, respectively, aiming to add 25 ml of $KMnO_4$ per 15 mg of organic C (calculated from $OC_{dichro}$ values). After 24 h shaking, the suspension was centrifuged at 2600 *g* for 1.5 h and the

extract decanted, after which the sediment was washed with distilled water until the supernatant was colorless. The MN in the residue was isolated and purified using 200 ml of 1 M NaOH for 24 h under $N_2$ atmosphere, analogous to the extraction of CR described above.

*2.4. Py-GC/MS*

Platinum filament Py-GC-MS was performed with a Pyroprobe 5000 (CDS Analytical Inc., Oxford, USA) coupled to a 6890 GC and 5975 MS (Agilent Technologies, Palo Alto, USA). The non-oxidized (NO) and oxidation-resistant SOM fractions (MN and CR) were pyrolyzed at 750 °C for 10 s (heating rate 10 °C/ms). Analyses of sample S2 of the CR series was repeated, first at 400 ºC and then at 750 ºC, to distinguish between evaporation and pyrolysis products from volatile and macromolecular components, respectively. The pyrolysis interface was set at 300 ºC and the GC inlet at 325 °C. The oven of the GC was heated from 50 to 325 °C at 10 °C/min and held isothermal for 5 min. The GC/MS transfer line was held at 325 °C, the ion source (in electron impact mode, 70 eV) at 230 °C and the quadrupole detector at 150 °C, measuring fragments in the *m/z* 50-500 range. The GC was equipped with a (non-polar) HP-1 100% dimethylpolysiloxane column. Helium was used as the carrier gas (constant gas flow, 1 ml/min). The major peaks in the total ion current of all samples were listed and, if possible, identified using the NIST ‘05 library and Py-GC/MS literature (Appendix A). Quantification of these pyrolysis products, 172 in total, was obtained by using the peak area of the major fragment ions (m/z). The sum of these peaks, i.e. total quantified peak area (TQPA) was set as 100% and the relative proportions of the pyrolysis products were calculated as the % of TQPA. This is a semi-quantitative estimate that allows for better comparison among samples than visual

inspection of pyrolysis chromatograms (pyrograms) alone, and produces a dataset that can be treated statistically.

### 2.5. *$^{13}$C NMR spectroscopy*

Solid-state NMR spectroscopy experiments were performed with cross-polarization magic angle spinning (CPMAS) at 298 K in a 17.6 T Varian Inova-750 spectrometer (operating at 750 MHz proton frequency) equipped with a T3 Varian solid probe [Varian, Inc, USA]. Solid NMR samples were prepared in 3.2 mm rotors with an effective sample capacity of 22 µL which corresponds to approximately 30 mg of the powdered sample. Spectra were processed and analyzed with MestreC software (Mestrelab Research Inc.). Carbon chemical shifts were referred to the carbon methylene signal of solid adamantane at 28.92 ppm. This sample was also used for the calibration of the 1D CPMAS experiments. 1D CPMAS spectra were acquired for the samples with the following conditions: the inter-scan delay was set to 0.5 s, the number of scans was 24000 and the MAS rate was 20 kHz. Heteronuclear decoupling during acquisition of the FID was performed with Spinal-64 with a proton field strength of 70 kHz. The cross polarization time was set to 1 ms. During cross polarization, the field strength of the proton pulse was set constant to 75 kHz and that of the $^{13}$C pulse was linearly ramped during a 10% of the duration with a 20 kHz ramp near the matching sideband. Spectra were divided into different regions of chemical shift following Knicker et al (2005). Relative abundances of the various C groups were determined by integration of the signal intensity in their respective chemical shift regions. The region between 0– 45 ppm is assigned to alkyl C corresponding to terminal methyl groups and methylene groups of aliphatic moieties. The *O*-alkyl C region, typically assigned to carbohydrate-derived structures, between 45– 95 ppm. Here, between 45– 60 ppm, *N*-

alkyl C (i.e. in amino sugars and peptide structures) can contribute to the signal. Between 90 and 160 ppm resonance lines of olefins and aromatic C are detected. The regions from 160 to 220 ppm and from 220 to 245 are assigned to carbonyl C separated into carboxyl/amide and aldehyde/ketone groups, respectively. Although often assumed that solid- state $^{13}C$ NMR underestimate BC, recent studies demonstrated that most charcoals have an atomic H/C ratio > 0.5 and thus provide sufficient protonation for efficient cross polarization and reliable NMR spectra (Knicker et al. 2005). Because of the limited sample availability some samples required Al-oxide to fill the rotor, causing some signal quality deterioration. Samples MN-2, MN-3 and CR-3 were not analyzed for that reason.

*2.6. Factor analysis*

The relative proportions of pyrolysis products were subjected to factor analysis using Statistica Version 8 (Statsoft, Tulsa, USA). Factor analysis proved useful in the interpretation of Py-GC/MS datasets, especially with respect to the sources and degradation states to which the pyrolysis products correspond.

## 3. Results and discussion

*3.1. Py-GC/MS: source allocation*

The pyrolysis products were grouped according to their chemical structure into the following classes: (i) aliphatic compounds (homologous series of *n*-alkanes and *n*-alkenes, and branched alkenes), (ii) lignin-derived methoxyphenols, (iii) phenols, (iv) monocyclic aromatic compounds (MAHs), (v) polycyclic aromatic hydrocarbons (PAHs), (vi) N-containing compounds, (vii) carbohydrate-derived pyrolysis products

and (viii) unidentified compounds. Appendix A is a list of the pyrolysis products identified.

*Aliphatic compounds.* *n*-alkane/*n*-alkene pairs, ranging from $C_{10}$ to $C_{28}$, originate largely from aliphatic biopolymers (Eglinton and Hamilton 1967). The other short- and mid-chain (ca. $C_{10}$-$C_{20}$) alkenes, not from the homologous series and most of which are probably branched, are considered significant products of charred aliphatic matter according to recent studies, even though they are not produced exclusively from pyrolysis of BC (Eckmeier and Wiesenberg 2009; Kaal et al. 2012a). Several *n*-fatty acids (mainly $C_{16}$ and $C_{18}$) seemed to increase disproportionally upon chemical oxidation, especially in CR. This might be explained by the enrichment of aliphatic structures upon dichromate oxidation due to their hydrophobicity (Knicker et al. 2007). However, the use of a HP-1 column, which has a larger internal diameter than frequently used non-polar columns for Py-GC/MS, may have affected the 'chromatographic mobility' and the relative proportions of these compounds, thus making its interpretation difficult. Therefore, these compounds were not included in the statistical analyses neither.

*Lignin-derived methoxyphenols.* Methoxyphenols (guaiacyl- and syringyl-based) are typical products of coniferyl and sinapyl lignin, respectively (Boerjan et al. 2003). 4-vinylphenol was also added to this group because it has frequently been shown to be marker of coumaryl lignin and the non-lignin coumaric acid in grasses (Sáiz-Jiménez and de Leeuw 1986). An unknown proportion of 4-vinylphenol and 4-vinylguaiacol may originate from non-lignin phenolic acids as well (Schellekens et al. 2012), but that does not influence the interpretation of results here as statistically they behave as the lignin markers (see below).

283 *Phenols*. The other phenols have multiple origins: phenol and $C_1$-$C_2$-
284 alkylphenols may originate from any phenolic precursor including lignin, tannin,
285 proteinaceous biomass, weakly-charred BC and carbohydrates (Tegelaar et al. 1995;
286 Stuczynski et al. 1997), while lignin, tannin or thermally demethylated lignin (Kaal et
287 al. 2012b) are the most likely precursors of 1,2-benzenediol (catechol).
288 *Monocyclic aromatic hydrocarbons*. MAHs include benzene, toluene, styrene,
289 dimethylbenzenes, linear $C_2$-$C_4$-alkylbenzenes, a dimethylstyrene and a dimethyl-
290 methylethylbenzene compound. MAHs are formed from many aromatic and some non-
291 aromatic precursors (Schulten et al. 1991) but BC is known to produce an exceptionally
292 high proportion of especially benzene (Kaal et al. 2012a). Indeed, the analysis of the
293 products of incomplete combustion by Py-GC/MS showed that MAHs and also PAHs
294 are major pyrolysis products of Black C (Pastorova et al. 1994, Almendros et al. 2003).
295 Besides a renewed interest in the detection of burning residues in SOM established that
296 BC is a major source of SOM and that its oxidation products could be a potential source
297 of highly aromatic humic acids (Hatcher et al. 1989; Skjemstad et al. 1996; Shindo et
298 al., 2004). On the other hand, the alkylstyrenes most likely originate from the
299 monoterpenes present in *Eucalyptus globulus* litter (see below).
300 *Polycyclic aromatic hydrocarbon compounds*. The origin of PAHs in SOM
301 pyrolyzates have been the subject of considerable debate. They were sometimes
302 considered actual building blocks of humic substances formed upon condensation
303 reactions during humification (Schulten et al. 1991), or more frequently interpreted as
304 analytical artefacts because of evidence of their formation during pyrolysis of aliphatic
305 compounds through cyclization and aromatization (Sáiz-Jiménez 1994b). More
306 recently, PAHs and particularly the non-alkyl-substituted and >2 ring PAHs (Rumpel et
307 al. 2007) are considered indicative of (but not markers of) BC in SOM (Kaal and

Rumpel 2009; Song and Peng 2010). In the present study, unsubstituted PAHs (indene, naphthalene, fluorene, biphenyl, phenanthrene and anthracene) and $C_1$-$C_2$ alkyl analogues of these PAHs were abundant. In addition, a series of $C_3$-$C_4$ alkylnaphthalenes and $C_{5:0}$ and $C_{5:1}$ alkylnaphthalenes probably originate from evaporation and pyrolysis of monoterpenes (e.g. pinene, phellandrene, eucalyptol) and sesquiterpenoids (aromadendrene, globulol), respectively, present in *Eucalyptus* sp. oil. Indeed, these compounds were identified in *Eucalyptus globulus* litter (a mixture of leaves, cortex and branches) pyrolyzates (data not shown). Some of the polysubstituted PAHs ($C_3$-indene, $C_2$-$C_{5:0}$- and $C_{5:1}$-naphthalene) provided the largest contributions to the pyrograms of sample S1 (contrary to many unsubstituted or $C_1$- alkylsubstituted PAHs, largely from BC); this suggests that a significant portion of these compounds originate from fresh *Eucalyptus* sp. litter. Overall, it should be noted that, in this study, where distinguishing between BC and non-pyrogenic SOM components will appear to be important, the interpretation of MAHs and PAHs relies more strongly on the growing body of knowledge on BC's pyrolysis fingerprints (Kaal et al. 2012a; Fabbri et al. 2012; Song and Peng 2010) than on previous studies on the structural characteristics of humic acids (Schulten et al. 1991; Sáiz-Jiménez 1994a).

*N-containing products*. Of the 24 N-containing pyrolysis products identified, benzonitrile and $C_1$-benzonitriles were recently proposed as the main products of N-containing groups in BC (Schnitzer et al. 2007; Song and Peng 2010). In addition, isoquinoline, phenylpyridine, benzenedicarbonitriles and pyridinecarbonitriles can be considered as markers of 'Black N' (BN) (Knicker 2007; Kaal et al. 2009). Note that absence of these products does not imply absence of BN: these compounds can probably only be detected in high-quality pyrograms of exceptionally BN-rich samples. Pyrroles, pyridines and indoles are potential products of BN as well but these

compounds are common in the pyrolyzates of non-pyrogenic N-moieties. Several markers of chitin (acetamide and a compound tentatively identified as trianhydro-2-acetamido-2-deoxyglucose; van der Kaaden et al. 1984; Stankiewicz et al. 1996) and chitin-entangled protein (diketopiperazine) probably originate from fungal cell walls and/or arthropod exoskeleta, either way serving as an indication of biologically re-assimilated ("secondary") remains in SOM (Gutierrez et al. 1995). Finally, for picolinamide, cyanobenzoic acid and phthalimide-based compounds no specific origin has been identified yet.

*Carbohydrate compounds*. Of the carbohydrate products identified, levoglucosan, dianhydro-α-glucopyranose, pyranones and dianhydrorhamnose largely originate from "fresh" or well-preserved polysaccharides (Stuczynski et al. 1997; Poirier et al. 2005; Nierop et al. 2005). On the other hand, cyclopentenediones, furans, furfurals, levoglucosenone and dibenzofuran originate from fresh and/or degraded carbohydrates (Buurman and Roscoe 2011). This degradation may be either biological or thermal in nature, the latter especially for the furans, furaldehydes and dibenzofuran (Pastorova et al. 1994; Boon et al. 1994).

*Unidentified compounds*. An unsaturated non-aromatic cyclic compound (U1) was identified only in the pyrolyzates from S1 (NO-1 and MN-1), which also contained the pollen of *Eucalyptus* sp. It probably corresponds to α-phellandrene, which is abundant in eucalyptus oils (Samaté et al. 1998). Furthermore, several polymethyl-substituted polycyclic compounds (U3-U6), also detected in the aforementioned fresh eucalyptus-litter pyrolyzate, probably derived from *Eucalyptus* sp. Finally, a methylated cyclohexane (U2) of unknown origin was tentatively identified.

### *3.2. Py-GC/MS: quantification and interpretation*

Pyrograms of chemical oxidation resistant SOM fractions and non-oxidized samples are represented in Fig. 1. The relative contributions to TQPA for identified groups in the different soil horizons studied are presented in Table 2. In NO-1, carbohydrate-derived pyrolysis products accounted for 30% of TQPA, with levoglucosan (Ps13) from intact polysaccharide (Stuczynski et al. 1997; Poirier et al. 2005) being dominant. The presence of 4-hydroxy-5,6-dihydro-(2H)-pyranone (Ps6) and dianhydrorhamnose (Ps7) confirms the existence of fresh (or well-preserved) polysaccharides in NO-1 (Nierop et al. 2005). Of the samples studied, these compounds showed the largest contribution to sample NO-1. The same pattern was observed for many other indicators of fresh plant material, including the aliphatic compound producing *m*/*z* 83+280, diketodipyrrole, and the lignin-derived products (Suárez-Abelenda et al. 2011). The large proportion of phenols in the pyrolyzate of this sample may be explained by the abundance of lignin. Samples NO-1 and MN-1 had the highest contributions of probably eucalyptus-derived moieties ($C_{5:0}$-, $C_{5:1}$-alkylnaphthalenes and α-phellandrene and $C_3$- naphthalenes). It is concluded that the SOM of NO-1 is characterized by a large fraction of well-preserved polysaccharides and lignin, with an additional contribution of specific eucalyptus-derived substances, and relatively small proportions of microbial and pyrogenic SOM. The latter is supported by the low benzene/alkyl-benzenes and PAH/alkyl-PAHs ratios (Table 2), which are indicative of a low contribution of strongly charred BC to the MAHs and PAHs of these samples (Kaal and Rumpel 2009; Kaal et al. 2012a).

Unsurprisingly, sample NO-2 (ca. 5,000 yr old), produced fewer pyrolysis products from fresh SOM than NO-1. More specifically, in comparison with NO-1, among the carbohydrate markers there was a strong increase of furans, furaldehydes, levoglucosenone and acetic acid, while levoglucosan, pyranones and

dianhydrorhamnose diminished, which is a clear indication of a shift of fresh polysaccharide to degraded/microbial carbohydrates (Sáiz-Jiménez and de Leeuw 1986; Buurman and Roscoe 2011). Lignin markers were virtually absent. NO-2 sample produced many N-compounds, including those from chitin (N3 and N22), pyridine (N1, often associated with microbial SOM; Buurman et al. 2007) and BN (e.g. aromatic carbonitriles and phenylpyridine). It also gave higher proportions of MAHs and BC-derived PAHs than the NO-1 sample. It is concluded that the SOM of sample NO-2 was predominantly composed of degraded/microbial and pyrogenic material.

The pyrolyzate of sample NO-3 was dominated by carbohydrate markers, with acetic acid, 3/2-furaldehyde, 5-methyl-2-furaldehyde, dianhydro-α-glucopyranose, a furanone and 4-acetylfuran accounting for 62% of TQPA (Table 2). These pyrolysis products are frequently ascribed to SOM with large proportions of microbial biomass (Sáiz-Jiménez and de Leeuw 1986; Buurman and Roscoe 2011). The small relative proportions of MAHs and PAHs suggest that BC accounts for only a minor portion of the SOM in NO-3. This is supported by the low ratios of benzene/alkyl-benzenes and PAH/alkyl-PAH (Table 2).

In general, the differences in pyrolyzate compositions between NO-samples and MN-samples were small, yet some are worth mentioning. For sample S1, oxidation with $KMnO_4$ (which promoted a decreased of 2.3 mg $g^{-1}$ of OC; Table1) caused an increase in MAHs (from 16.4% in NO-1 to 30.0% in MN-1) and decrease in carbohydrates (from 30.4% to 18.4%) and lignin (from 7.4% to 3.0 %) (Table 2). These results can be explained by the partial oxidation of fresh SOM (van Soest and Wine 1986; Tirol-Padre and Ladha 2004) and the relative enrichment of pyrogenic (Almendros et al. 1990) and aliphatic SOM (González-Vila and Martín 1985; Almendros et al. 1989). Besides, permanganate oxidation concentrates pyrolysis products from aromatic structures

present in humic acids in general (Polvillo et al. 2009), even though cyclization of aliphatic precursors may play a role as well (González-Vila and Martín 1985). In sample S2, $KMnO_4$ oxidation (MN-2) (with a smaller decrease of OC; 1.3 mg $g^{-1}$) caused a strong decline in carbohydrate products (from 31.5% to 17.4% of TQPA in NO-2 and MN-2, respectively) and an increase in aliphatic pyrolysis products (sum of *n*-alkanes, *n*-alkenes and other aliphatic compounds from 5.3% in NO-2 to 23.1% in MN-2). These changes are indicative of selective oxidation of (an unknown proportion of) the degraded/microbial SOM and the relative enrichment of aliphatic precursors probably from degraded root components (Kaal and van Mourik 2008). In addition, MN-2 produced higher amounts of N-containing BC markers, as BC and BN are relatively resistant against oxidation with this reagent. Skjemstad et al. (2006) found that $KMnO_4$ may react significantly with BC, but no evidence of this was found here. Finally, sample MN-3 (with a decrease of 1.7 mg $g^{-1}$ of its OC content) contains a smaller proportion of carbohydrates than NO-3 (17.7% vs. 62.2% of TQPA), confirming that the degraded/microbial carbohydrate fraction is relatively susceptible to this oxidation agent.

The pyrolyzates obtained from the residues after dichromate oxidation were very different from those of NO- and MN-samples. The CR-1 sample (27.5 mg $g^{-1}$ of its OC was oxidized by dichromate; Table 1) was strongly enriched in aliphatic pyrolysis products (34% of TQPA), particularly of short-chain ($<C_{18}$) *n*-alkanes/*n*-alkenes (located on the right side of the broken line in the aliphatic cluster; SE quadrant, Fig. 2) and branched alkenes, and depleted in lignin-, carbohydrate- and eucalyptus-derived pyrolysis products in comparison with NO-1 and MN-1. CR-1 also produced the highest proportions of 3-ring PAHs and higher ratios of benzene/alkyl-benzenes and PAH/alkyl-PAHs ratios (Table 2), suggesting that a large proportion of the MAHs and

PAHs from the CR-1 is pyrogenic. These results are indicative of the enrichment of pyrogenic SOM in the fraction resistant to $K_2Cr_2O_7$- oxidation. Indeed, the partial resistance of BC to $K_2Cr_2O_7$ oxidation is well-documented (Knicker et al. 2007, 2008). The same studies showed the existence of a $K_2Cr_2O_7$-resistant alkyl fraction (Knicker et al. 2007, 2008), which was also supported by the pyrolyzate composition of CR-1. The increase was also observed for the *n*-fatty acids (data not shown), which are not considered part of structural aliphatic plant material. These results support the hypothesis that the enrichment of aliphatic material in the residual fraction of the $K_2Cr_2O_7$ oxidation residues is produced by the hydrophobic nature of these constituents (Knicker et al. 2007), possibly in combination with chemical recalcitrance of C-C bonds in methylene chains. Finally, a decrease was observed for the intact terpene-like plant-derived PAHs, clearly showing different origin for the un- and methyl-substituted PAHs (mainly from BC) and the polyalkyl-substituted PAHs from eucalyptus litter. For sample CR-2, dichromate oxidation oxidized less OC (12.3 mg $g^{-1}$ for CR-2) than for CR-1. It produced a further decrease in the proportion of lignin markers in comparison with MN-2, and of microbial products such as acetamide and furans, while the BC and BN fingerprints were relatively intense (e.g. benzene, unsubstituted PAHs, benzene carbonitriles, isoquinoline and dibenzofuran). The largest proportion of these BC-derived pyrolysis products coincides with the highest macroscopic charcoal content of sample S2 (Table 1). These results confirm the accumulation of BC and BN in the residues after $K_2Cr_2O_7$ oxidation. Similar to CR-1, sample CR-2 was enriched in aliphatic pyrolysis products. Unexpectedly, significant amounts of the markers of well-preserved polysaccharides such as levoglucosan, were detected in the pyrolyzates of CR-2 and CR-3. With the information available at this moment, our best explanation to this observation is the presence of an uncharred cellulose-containing core (Knicker et al.

2005) in incompletely charred particles and thereby protected against $K_2Cr_2O_7$ oxidation. Sample CR-3 (in which dichromate caused a loss of 14.3 mg $g^{-1}$ of OC) was also enriched in pyrogenic SOM with a high contribution of BN markers, and in an aliphatic component with particularly high contributions of branched alkenes from an aliphatic SOM fraction, possibly in part pyrogenic.

*3.3. Py-GC/MS: factor analysis*

The first four factors (F1-F4) explained 81% of the variation in the Py-GC/MS dataset, with F1 and F2 combined accounting for 61%. The loadings of the pyrolysis products, and the scores of the samples analyzed, are shown in F1-F2 factor space (Fig. 2).

*n*-Alkanes/ *n*-alkenes are predominantly represented in the SE quadrant with high positive loadings on F1. Lower loadings on F1 were observed for the *n*-alkenes >$C_{20}$ than for $C_{10}$-$C_{20}$ *n*-alkenes. Branched alkenes plot between their straight-chain analogues and the pyrogenic SOM markers, supporting the hypothesis that these branched alkenes are associated with charred aliphatic precursors (Eckmeier and Wiesenberg 2009; Kaal and Rumpel 2009).

The N-containing compounds are spread throughout the F1-F2 factor space, which is a result of the diverse origin of the members of this group. One cluster of N-containing compounds in the NE quadrant is composed of benzonitrile, $C_1$-benzonitriles, benzene dicarbonitriles, cyanobenzoic acid, pyridine, $C_1$-pyridine and pyridinecarbonitrile, clearly reflecting a pyrogenic origin. Indeed, many non-alkyl-substituted PAHs and dibenzofuran, also associated with BC (Pastorova et al. 1994), plot in the same region. Chitin-derived N compounds (chitin markers such as acetamide) and 4-acetylfuran are spread out in the NW quadrant together with microbial

polysaccharides whilst diketodipyrrole denotes the presence of fresh SOM in the SW quadrant (see below). Indoles are spread throughout the SW and SE quadrants, which may be indicative of a mixed origin.

The lignin-derived products (including free phenolic acids), i.e. 4-vinylphenol, guaiacols and syringols), and catechol occur in the SW quadrant together with an aliphatic marker of fresh plant material (Al13). Most of the remaining pyrolysis products in this region are associated with fresh or well-preserved SOM components as well: phenol and alkylphenols (in this case from lignin), $C_{5:0}$ and $C_{5:1}$ alkylnaphthalenes (from eucalyptus litter), dianhydrorhamnose (from polysaccharides) and diketodipyrrole and indoles (typical N-containing pyrolysis products of fresh proteinaceous biomass; Buurman and Roscoe 2011). Levoglucosan plots between fresh OM and charred material; this may be attributed to the aforementioned protection of cellulose in interior parts of charcoal particles in dichromate oxidation residues or an unknown alternative levoglucosan source. The other carbohydrate products are spread along F2 because they have multiple sources, most of which corresponding to degraded/microbial SOM. The carbohydrate products of degraded/microbial SOM are probably those that plot in the NW quadrant: furans (4-acetylfuran, 3/2-furaldehyde and 5-methyl-2-furaldehyde), glucopyranose, which is microbial marker (Nierop et al. 2005), and acetic acid. This interpretation is consistent with the presence of the markers of chitin in this region of factor space.

In summary, F1-F2 separates the pyrolysis products according to their principal origin. Factor 1 separates the pyrogenic and aliphatic oxidation-resistant SOM fractions (chemically stable) from the fresh and degraded SOM fractions (chemically labile), while decomposed and pyrogenic SOM (strongly altered) are separated from fresh and

oxidation-resistant aliphatics (resembling plant material) according to their loadings on F2.

The factor scores of the samples can be used to identify the main differences between the samples analyzed (Fig. 2). As such, the samples with a large fraction of fresh biomass (NO-1 and MN-1) plot in the SW quadrant. Sample CR-1 plots in the SE quadrant, as dichromate oxidation eliminated most of the fresh SOM causing the relative accumulation of aliphatic SOM and weakly charred material. Sample S2 is a mixture of mainly degraded SOM and BC (with small contributions of fresh and aliphatic material), which is why NO-2 plots in the NW region, dominated by degraded/microbial markers, while MN-2 and CR-2 plot in the NE quadrant because of relative enrichment of BC after chemical treatment. Sample S3 was also rich in microbial SOM but has a lower content of chemically recalcitrant/hydrophobic aliphatic SOM and BC, and higher proportion of degraded/microbial SOM; this explains why NO-3 has a high F2 score while MN-3 and CR-3 plot in the NE quadrant reflecting BC enrichment after the selective depletion of degraded/microbial SOM. The short distance in factorial space between MN-3 and CR-3, and the large distance between these samples and NO-3, suggests a that the abundant degraded/microbial biomass (carbohydrates, chitin) in this sample is highly susceptible to permanganate and dichromate treatment.

From these results some inferences on the effects of the oxidation agents on SOM composition can be made. First, the minor differences between NO-1 and MN-1 can be explained by the relatively small microbial contribution to sample S1. In contrast, $K_2Cr_2O_7$ thoroughly modified the pyrolysis fingerprint obtained from the residues of S1 by eliminating lignin, polysaccharides and terpenes, and relative enrichment of aliphatic and pyrogenic structures. In the older samples, where the aliphatic fraction is less

dominant while that of degraded/microbial and pyrogenic SOM prevail, chemically oxidized samples (MN-2, MN-3, CR-2 and CR-3) had positive scores on F1 and F2 mainly because both oxidants concentrate BC, with $K_2Cr_2O_7$ being the stronger oxidant.

*3.4. Solid- state $^{13}C$ NMR spectroscopy: results and comparison with Py-GC/MS*

Samples are compared by relative intensity of the chemical shift regions. The spectrum of NO-1 (Fig. 3) was characterized by a dominant signal at 21 ppm and a shoulder at 29 ppm (combined 29%, Table 3) from alkyl C, which can be ascribed to aliphatic structures in fatty acids, lipids, waxes, cutan, suberan, cutin and suberin (Tegelaar et al. 1989) but also peptide structures and short alkyl side-chains. In the *O*-alkyl C region (45–110 ppm) a broad peak at 75 ppm (with a contribution of 29%) was detected, which is generally attributed to cellulose, hemicelluloses and pectins (Gramble et al. 1994; Kögel-Knabner 1997). The peak at 55 ppm probably corresponds to methoxyl groups in lignin structures (Kögel-Knabner 1997) but can also have contributions of *N*-alkyl from amino sugars and peptides. The *O*-substituted aromatic C between 140- 160 ppm may derive from lignin and oxidized BC (Knicker et al. 2005). Resonance lines of aromatic C-H groups are detected in the chemical shift region between 110 ppm and 140 ppm (14%) (Knicker and Lüdemann 1995). The chemical shifts of carbon in carboxylic acids, esters and amides fall within the range between 160 ppm and 220 ppm and represents 15% of the total $^{13}C$ intensity. There are minor contributions of carbonyl or aldehydes, giving signals between 220- 245 ppm.

The NMR spectra of NO-2 and NO-3 differ considerably from that of NO-1. In NO-2, the *O*-alkyl C fraction has the highest values (26%), followed by alkyl C, carboxyl/amide C and aromatic C. Considering that there is no clear signal in the O-substituted C region (from 140– 160 ppm), this spectrum can be best explained with a

considerable contribution of oxidized charcoal. NO-3 presented the highest contribution of non-lignin aromatic fraction, probably BC-derived (31%) and a large signal of carboxyl/amide C (26%), which likely originates from microbial compounds.

The chemical oxidants had several effects on the NMR signal obtained from sample S1. After the $KMnO_4$ treatment (MN-1), and comparable to results from Py-GC-MS, a spectrum similar to that of NO-1 but with slightly higher relative intensities in the alkyl C (34%) region was acquired, confirming other $^{13}C$ NMR studies (Tirol-Padre and Ladha 2004) in that cellulose is largely resistant to permanganate oxidation. Dichromate oxidation of sample S1 caused an increase of the relative contribution of aromatic C (sum of aromatic C-H and aromatic C-O-R) (from 17% in NO-1 to 25% in CR-1) with a concomitant depletion of methoxyl C/*N*-alkyl C and *O*-alkyl C (see Table 3). Note that differences between NO-1 and CR-1 by NMR are smaller than observed by Py-GC/MS. This indicates that, as Py-GC/MS data seem to be best supported, NMR results must be taken carefully.

The spectrum of CR-2 showed the highest intensity in the chemical shift region of aromatic C (45%). Considering the absence of methoxyl C signal, the width of the signal band (from 90 to 140 ppm) and the composition of the pyrolysis fingerprint, this aromatic signal originates from BC (see also Skjemstad et al. 1996; Knicker et al. 2005). Moreover, the contribution of alkyl C was strongly reduced upon $K_2Cr_2O_7$ oxidation (10% in CR-2).

In summary, in NO samples, $^{13}C$ NMR spectroscopy shows a relative decrease with depth of aliphatic C, carbohydrates and lignin moieties and a relative increase with depth of a non-lignin aromatic fraction (probably BC) and carboxyl/amide C (possibly oxidized BC in combination with N-rich microbial SOM), which is in agreement with Py-GC/MS data. With regard to the effects of chemical oxidation, both Py-GC/MS and

582 $^{13}C$ NMR spectroscopy showed a decrease of easily degradable SOM (mainly composed
583 of fresh lignin and polysaccharides) and an increase of the aromatic fraction. Besides,
584 lignin was slightly oxidized by $KMnO_4$ contrary to that observed by previous studies
585 (van Soest and Wine 1986; Tyrol-Padre and Ladha 2004; Skjemstad et al. 2006) where
586 lignin was strongly degraded. The increase of aliphatic moieties upon chemical
587 oxidation, as suggested by Py-GC/MS, was also observed by NMR spectroscopy in the
588 superficial sample S1 although it strongly decreased in S2. However here one has to
589 bear in mind that the alkyl C region does not only contain intensity of lipids but have
590 considerable contributions of peptide structures or short alkyl side-chains (such as $C_3$-
591 side chains in lignin). Those moieties may be expected to be relatively susceptible to
592 oxidation resulting in a relative depletion of the signal intensity in the alkyl C region
593 even though longer chain aliphatic components may have experienced a relative
594 enrichment.
595
596 **4. Conclusions**
597 The molecular study of SOM fractions of three horizons of a colluvial soil
598 representing ages of 100, 5,000 and 9,700 yr, before and after treatment with $KMnO_4$
599 and $K_2Cr_2O_7$, provided detailed information on SOM composition (with regard to
600 source and degradation/preservation state) and the behaviour of different SOM fractions
601 towards these oxidation agents. *Eucalyptus*-derived terpenes and sesquiterpenes were
602 only present in the youngest sample and resisted $KMnO_4$ but not $K_2Cr_2O_7$ oxidation.
603 Microbial/degraded SOM, mostly composed of carbohydrates and chitin, was especially
604 abundant in the deeper layers of the soil and appeared highly susceptible to both
605 $KMnO_4$ and $K_2Cr_2O_7$ oxidation. As such, $KMnO_4$ could be used as an indication of the
606 abundance of microbial biomass. Both oxidants, $K_2CR_2O_7$ in particular, concentrated

two other SOM fractions abundant in this soil: aliphatic and pyrogenic material (BC), the latter having a significant amount of N-containing functional groups (BN). These fractions probably survived $K_2Cr_2O_7$ oxidation because of the chemical stability of polyaromatic moieties (BC) and resistant C-C bonds in methylene chains and/or hydrophobicity of the aliphatic fraction (which is probably root-derived). It appeared that especially $K_2Cr_2O_7$ oxidation efficiently concentrates BC and oxidation-resistant aliphatic structures from other SOM sources, and that in combination with Py-GC/MS it is possible to distinguish between these sources (yet not quantitatively) while $^{13}C$ NMR may assist in obtaining estimations of their relative proportions. Finally, BC isolation by dichromate oxidation and posterior quantification through total digestion (Knicker et al., 2007) is discouraged as a significant aliphatic fraction resists dichromate producing an overestimation of its contents.

**Acknowledgements**

We thank Antonio Martínez-Cortizas for the discussion on the statistical analysis. The contribution of M. Camps-Arbestain to this research was funded by MAF and NZAGRC. The authors also thank the anonymous reviewers for their constructive comments on the manuscript.

**References**

Almendros G, González-Vila FJ, Martin F, (1989) Room temperature alkaline permanganate oxidation of representative humic acids. *Soil Biology and Biochemistry* **21**, 481–486.

630 Almendros G, González-Vila FJ, Martin F (1990) Fire-induced transformation of soil
631 organic matter from an oak forest: an experimental approach to the effects of fire
632 on humic substances. *Soil Science* **149**, 158–168.

633 Almendros G, Knicker H, González-Vila FJ (2003) Rearrangement of carbon and
634 nitrogen forms in peat after progressive thermal oxidation as determined by solid-
635 state $^{13}$C- and $^{15}$N NMR spectroscopy. *Organic Geochemistry* **34**, 1559–1568.

636 Baldock JA, Smernik RJ (2002) Chemical composition and bioavailability of thermally
637 altered Pinus resinosa (Red pine) Wood. *Organic Geochemistry* **33**, 1093–1109.

638 Boerjan W, Ralph J, Baucher M (2003) Lignin biosynthesis. *Annual Review of Plant*
639 *Physiology and Plant Molecular Biology* **54**, 519–546.

640 Boon JJ, Pastorova I, Botto RE, Arisz PW (1994) Structural studies on cellulose
641 pyrolysis and cellulose chars by PYMS, PYGCMS, FTIR, NMR and by wet
642 chemical techniques. *Biomass and Bioenergy* **7**, 25–32.

643 Buurman P, Petersen F, Almendros G (2007) Soil organic matter chemistry in
644 allophanic soils: A pyrolysis-GC/MS study of a Costa Rican Andosol Catena.
645 *European Journal of Soil Science* **58**, 1330–1347.

646 Buurman P, Roscoe R (2011) Different chemistry of free light and occluded light and
647 extractable SOM fractions in soils of Cerrado, tilled and untilled fields, Minas
648 Gerais, Brazil - a pyrolysis-GC/MS study. *European Journal of Soil Science* **62**,
649 253–266.

650 Carballas T, Duchaufour P, Jacquin F (1967) Évolution de la matière organique des
651 rankers. *Bulletin de l'École Nationale Supérieure Agronomique de Nancy* **9**, 20–
652 28.

653 Christensen BT (1992) Physical fractionation of soil and organic matter in primary
654 particle size and density separates. In 'Advances in Soil Science, Volume 20'. (Ed
655 BA Stewart) pp. 1–90. (Springer: New York).

656 Conteh A, Lefroy RDB, Blair GJ (1997) Dynamics of organic matter in soil as
657 determined by variations in $^{13}C/^{12}C$ isotopic ratios and fractionation by ease of
658 oxidation. *Australian Journal of Soil Resources* **35**, 881–890.

659 Eckmeier E, Wiesenberg GLB (2009) Short-chain *n*-alkanes ($C_{16}$–$C_{20}$) in ancient soil
660 are useful molecular markers for prehistoric biomass burning. *Journal of*
661 *Archaeological Science* **36**, 1590–1596.

662 Eglinton G, Hamilton RJ (1967) Leaf epicuticular waxes. *Science* **156**, 1322–1335.

663 Eusterhues K, Rumpel C, Kleber M, Kögel-Knabner I (2003) Stabilisation of soil
664 organic matter by interactions with minerals as revealed by mineral dissolution
665 and oxidative degradation. *Organic Geochemistry* **34**, 1591–1600.

666 Eusterhues K, Rumpel C, Kögel-Knabner I (2005) Stabilization of soil organic matter
667 isolated via oxidative degradation. *Organic Geochemistry* **36**, 1567–1575.

668 Fabbri D, Torri C, Spokas KA (2012) Analytical pyrolysis of synthetic chars derived
669 from biomass with potential agronomic application (biochar). Relationships with
670 impacts on microbial carbon dioxide production. *Journal of Analytical and*
671 *Applied Pyrolysis* **93**, 77–84.

672 Fründ R, Haider K, Lüdemann HD (1993) Impacts of soil management practices on the
673 organic matter structure - investigations by CPMAS $^{13}C$ NMR-spectroscopy.
674 *Zeitschrift fur Pflanzenernährung und Bodenkunde* **157**, 29–35.

675 Gillman GP, Sinclair DF, Beech TA (1986) Recovery of organic carbon by the Walkley
676 and Black procedure in highly weathered soils. *Communications in Soil Science*
677 *and Plant Analysis* **17**, 885–892.

678 González-Vila FJ, Martin F (1985) Chemical structural characteristics of humic acids
679 extracted from composted municipal refuse. *Agriculture, ecosystems &*
680 *environment* **14**, 267–278.

681 Gramble GR, Sethuraman A, Akin DE, Eriksson KE (1994) Biodegradation of
682 lignocellulose in Bermuda grass by white rot fungi analysed by solid-state $^{13}C$
683 Nuclear Magnetic Resonance. *Applied Environmental Microbiology* **60**, 3138–
684 3144.

685 Gutierrez A, Martínez MJ, Almendros G, González-Vila FJ, Martínez AT (1995)
686 Hyphal-sheath polysaccharides in fungal deterioration. *The Science of the Total*
687 *Environment* **167**, 315–328.

688 Harvey OR, Kuo LJ, Zimmerman AR, Louchouarn P, Amonette JE, Herbert BE (2012)
689 An Index-Based Approach to Assessing Recalcitrance and Soil Carbon
690 Sequestration Potential of Engineered Black Carbons (Biochars). *Environmental*
691 *Science and Technology* **46**, 1415–1421.

692 Hatcher PG, Schnitzer M, Vassallo AM, Wilson MA (1989) The chemical structure of
693 highly aromatic humic acids in three volcanic ash soils as determined by dipolar
694 dephasing NMR studies. *Geochimica et Cosmochimica Acta* **53**, 125–130.

695 Heanes DL (1984) Determination of total organic-C in soils by an improved chromic
696 acid digestion and spectrophotometric procedure. *Soil Science and Plant Analysis*
697 **15**, 1191–1213.

IUSS Working Group WRB (2006) World Reference Base for Soil Resources. In 'World Soil Resources Reports No. 103, 2nd Edition'. (FAO: Rome).

Kaal J, van Mourik JM (2008) Micromorphological evidence of black carbon in colluvial soils from NW Spain. *European Journal of Soil Science* **59**, 1133–1140.

Kaal J, Rumpel C (2009) Can pyrolysis-GC/MS be used to estimate the degree of thermal alteration of black carbon? *Organic Geochemistry* **40**, 1179–1187.

Kaal J, Martínez-Cortizas A, Nierop KGJ (2009) Characterisation of aged charcoal using a coil probe pyrolysis-GC/MS method optimised for black carbon. *Journal of Analytical and Applied Pyrolysis* **85**, 408–416.

Kaal J, Carrión Y, Asouti E, Martín Seijo M, Costa Casais M, Martínez Cortizas A, Criado Boado F (2011) Long-term deforestation in NW Spain: Linking the Holocene fire history to vegetation change and human activities. *Quaternary Science Reviews* **30**, 161–175.

Kaal J, Schneider MPW, Schmidt MWI (2012a). Rapid molecular screening of black carbon (biochar) thermosequences obtained from chestnut wood and rice straw: a pyrolysis-GC/MS study. *Biomass and Bioenergy* **45**, 115–129.

Kaal J, Nierop KGJ, Kraal P, Preston CM (2012b) A first step towards identification of tannin-derived black carbon: conventional pyrolysis (Py-GC-MS) and thermally assisted hydrolysis and methylation (THM-GC-MS) of charred condensed tannins. *Organic Geochemistry* **47**, 99–108.

Kleber M, Mikutta R, Torn MS, Jahn R (2005) Poorly crystalline mineral phases protect organic matter in acid subsoil horizons. *European Journal of Soil Science* **56**, 717–725.

721 Kleber M (2010) What is recalcitrant soil organic matter?. *Environmental Chemistry* **7**,
722 320–332.

723 Knicker H, Lüdemann HD (1995) $^{15}N$ and $^{13}C$ CPMAS and solution NMR studies of
724 $^{15}N$ enriched plant-material during 600 days of microbial degradation. *Organic*
725 *Geochemistry* **23**, 329–341.

726 Knicker H, Totsche KU, Almendros G, González-Vila FJ (2005) Condensation degree
727 of burnt peat and plant residues and the reliability of solid-state VACP MAS $^{13}C$
728 NMR spectra obtained from pyrogenic humic material. *Organic Geochemistry* **36**,
729 1359–1377.

730 Knicker H (2007) How does fire affect the nature and stability of soil organic nitrogen
731 and carbon? A review. *Biogeochemistry* **85**, 91–118.

732 Knicker H, Müller P, Hilscher A (2007) How useful is chemical oxidation with
733 dichromate for the determination of "Black Carbon" in fire-affected soils?.
734 *Geoderma* **142**, 178–196.

735 Knicker H, Hilscher A, González-Vila FJ, Almendros G (2008) A new conceptual
736 model for the structural properties of char produced during vegetation fires.
737 *Organic Geochemistry* **39**, 935–939.

738 Kögel-Knabner I (1995) Composition of soil organic matter. In 'Methods in Applied
739 Soil Microbiology and Biochemistry'. (Eds P Nannipieri, K Alef) pp. 66–78.
740 (Academic Press: London)

741 Kögel-Knabner I (1997) $^{13}C$ and $^{15}N$ NMR spectroscopy as a tool in soil organic matter
742 studies. *Geoderma* **80**, 243–270.

743 Lefroy RDB, Blair GJ, Strong WM (1993) Changes in soil organic matter with cropping
744 as measured by organic carbon fractions and $^{13}C$ natural isotope abundance. *Plant*
745 *and Soi*l **155/156**, 399–402.

746 Loginow W, Wisniewski W, Gonet SS, Ciescinska B (1987) Fractionation of organic C
747 based on susceptibility to oxidation. *Polish Journal of Soil Science* **20**, 47–52.

748 López-Merino L, Silva-Sánchez N, Kaal J, López-Sáez JA, Martínez-Cortizas A (2012)
749 Post-disturbance vegetation dynamics during the Late Pleistocene and the
750 Holocene: an example from NW Iberia. *Global Planetary Change* **92/93**, 58–70.

751 Macías F, Camps Arbestain M (2010) Soil carbon sequestration in a changing global
752 environment. *Mitigation and Adaptation Strategies for Global Change* **15**, 511–
753 529.

754 Moldoveanu SC (1998) An introduction to analytical pyrolysis. In 'Analytical Pyrolysis
755 of Organic Polymers. Techniques and instrumentation in analytical chemistry'.
756 (Ed SC Moldoveanu) pp. 20. (Elsevier: Amsterdam).

757 Nelson DW, Sommers LE (1996) Total carbon, organic carbon, and organic matter. In
758 'Methods of Soil Analysis 2, 2nd ed'. (Eds DL Sparks, AL Page, PA Helmke, RH
759 Loeppert, PN, Soltanpour, MA, Tabatabai, CT, Johnston, ME Sumner) pp. 961–
760 1010. (American Society of Agronomy, Inc: Madison, WI).

761 Nierop KGJ, van Bergen F, Buurman P, van Lagen B (2005) NaOH and Na-$Na_4P_2O_7$-
762 extractable organic matter in two allophanic volcanic ash soils of the Azores
763 Islands-a pyrolysis GC/MS study. *Geoderma* **127**, 36–51.

764 Piccolo A (1996) Humus and soil conservation. In 'Humic Substances in Terrestrial
765 Ecosystems'. (Ed A Piccolo) pp. 225–264. (Elsevier: Amsterdam)

766 Pastorova I, Botto RE, Arisz PW, Boon JJ (1994) Cellulose char structure: a combined
767 analytical Py-GC-MS, FTIR and NMR study. *Carbohydrate Research* **262**, 27–
768 47.

769 Poirier N, Sohi SP, Gaunt JL, Mahieu N, Randall EW, Powlson DS, Evershed RP
770 (2005) The chemical composition of measurable soil organic matter pools.
771 *Organic Geochemistry* **36**, 136–151.

772 Polvillo O, González-Pérez JA, Boski T, González-Vila FJ (2009) Structural features of
773 humic acids from a sedimentary sequence in the Guadiana estuary (Portugal–
774 Spain border). *Organic Geochemistry* **40**, 20–28.

775 Rumpel C, González-Pérez JA, Bardoux G, Largeau C, González-Vila FJ, Valentín C
776 (2007) Composition and reactivity of morphologically distinct charred materials
777 left after slash-and-burn practices in agricultural tropical soils. *Organic*
778 *Geochemistry* **38**, 911–920.

779 Sáiz-Jiménez C, de Leeuw JW (1986) Chemical characterization of soil organic matter
780 fractions by analytical pyrolysis-gas chromatography-mass spectrometry. *Journal*
781 *of Analytical and Applied Pyrolysis* **9**, 99–119.

782 Sáiz-Jiménez C (1994a) Analytical pyrolysis of humic substances; pitfalls, limitations,
783 and possible solutions. *Environmental Science and Technology* **28**, 1173–1780.

784 Sáiz-Jiménez C (1994) Production of alkylbenzenes and alkylnaphthalenes upon
785 pyrolysis of unsaturated fatty acids. *Naturwissenschaften* **81**, 451–453.

786 Samaté AD, Nacro M, Menut C, Malaty G, Bessiere JM (1998) Aromatic plants of
787 tropical west Africa. VII. Chemical composition of essential oils of two
788 Eucalyptus species (Myrtaceae) from Burkina Fasso: Eucalyptus alba Muell. and

789 Eucalyptus camaldulensis Dehnardt. *Journal of Essential Oil Research* **10**, 321–
790 324.

791 Schellekens J, Buurman P, Kuyper TW (2012) Source and transformations of lignin in
792 Carex-dominated peat. *Soil Biology & Biochemistry* **53**, 32–42.

793 Schmidt MWI, Skjemstad JO, Czimczik CI, Glaser B, Prentice KM, Gelinas Y,
794 Kuhlbusch TAJ (2001) Comparative analysis of black carbon in soils. *Global*
795 *Biogeochemical Cycles* **15**, 163–167.

796 Schnitzer MI, Monreal CM, Jandl G, Leinweber P, Fransham PB (2007) The conversion
797 of chicken manure to biooil by fast pyrolysis II. Analysis of chicken manure,
798 biooils, and char by curie-point pyrolysis-gas chromatography/mass spectrometry
799 (Cp Py-GC/MS). *Journal of Environmental Science and Health* **42**, 79–95.

800 Schulten HR, Plage B, Schnitzer M (1991) A chemical structure for humic substances.
801 *Naturwissenschaften* **78**, 311–312.

802 Shindo H, Honna T, Yamamoto S, Honma H (2004). Contribution of charred plant
803 fragments to soil organic carbon in Japanese volcanic ash soils containing black
804 humic acids. *Organic Geochemistry* ***35***, 235–241.

805 Six J, Conant RT, Paul EA, Paustian K (2002) Stabilization mechanisms of soil organic
806 matter: Implications for C-saturation of soils. *Plant and Soil* 241, 155–176.

807 Skjemstad JO, Clarke P, Taylor JA, Oades JM, McClure SG (1996) The chemistry and
808 nature of protected carbon in soil. *Australian Journal of Soil Resources* **34**, 251–
809 271.

Skjemstad JO, Taylor JA (1999) Does the Walkley-Black method determine soil charcoal?. *Communications in Soil Science and Plant Analysis* **30**, 2299–2310.

Skjemstad JO, Swift RS, McGowan JA (2006) Comparison of the particulate organic carbon and permanganate oxidation methods for estimating labile soil organic carbon. *Soil Research* **44**, 255–263.

Soil Survey Staff (1998) 'Keys to Soil Taxonomy (8th ed.)'. USDA Natural Resources Conservation Sites (NRCS): Washington.

Song J, Peng P (2010) Characterisation of black carbon materials by pyrolysis-gas chromatography-mass spectrometry. *Journal of Analytical Applied Pyrolysis* **87**, 129–137.

Stankiewicz BA, van Bergen PF, Duncan IJ, Carter JF, Briggs DEG, Evershed RP (1996) Recognition of chitin and proteins in invertebrate cuticles using analytical pyrolysis/gas chromatography and pyrolysis/gas chromatography/mass spectrometry. *Rapid Communications in Mass Spectroscopy* **10**, 1747–1757.

Stevenson FJ (1994) 'Humus Chemistry, Genesis, Composition, Reactions 2nd ed'. (John Wiley and Sons: New York).

Stuczynski TI, McCarthy GW, Reeves JB, Wright RJ (1997) Use of pyrolysis GC/MS for assessing changes in soil organic matter quality. *Soil Science* **162**, 97–105.

Suárez-Abelenda M, Buurman P, Camps Arbestain M, Kaal J, Martínez-Cortizas A, Gartzia-Bengoetxea N, Macías F (2011) Comparing NaOH-extractable organic matter of acid forest soils that differ in their pedogenic trends: a pyrolysis-GC/MS study. *European Journal of Soil Science* **62**, 834–848.

832 Tabatabai MA (1996) Soil organic matter testing: an overview. In 'Soil organic matter:
833 Analysis and interpretation. SSSA Special Publication 46'. (Eds FR Magdoff, MA
834 Tabatabai, EA Hanlon) pp. 1–9. (SSSA: Madison, WI)

835 Tegelaar EW, de Leeuw JW, Sáiz-Jiménez C (1989) Possible origin of aliphatic
836 moieties in humic substances. *Science of the Total Environments* **81/82**, 1–17.

837 Tegelaar EW, Hollman G, Vandervegt P, de Leeuw JW, Holloway PJ (1995) Chemical
838 characterization of the periderm tissue of some angiosperm species: Recognition
839 of an insoluble, nonhydrolyzable, aliphatic biomacromolecule (suberan). *Organic*
840 *Geochemistry* **23**, 239–251.

841 Tirol-Padre A, Ladha JK (2004) Assessing the reliability of permanganate- oxidizable
842 carbon as an index of soil labile carbon. *Soil Science Society of America Journal*
843 **68**, 969–978.

844 van der Kaaden A, Boon JJ, de Leeuw JW, de Lange F, Wijnand Schuyl PJ, Schulten
845 HR, Bahr U (1984) Comparison of analytical pyrolysis techniques in the
846 characterization of chitin. *Analytical Chemistry* **56**, 2160–2165.

847 van Soest PJ, Wine RH (1986) Determination of lignin and cellulose in acid-detergent
848 fibre with permanganate. *Journal of the Association of Official Agricultural*
849 *Chemists* **51**, 780–785.

850 Wilson MA, Barron PF, Goh KM (1981) Cross polarisation $^{13}C$ NMR spectroscopy of
851 some genetically related New Zealand soils. *Journal of Soil Science* **32**, 419–425.

852 Wolbach WS, Anders E (1989) Elemental carbon in sediments: Determination and
853 isotopic analysis in the presence of kerogen. *Geochimica et Cosmochimica Acta*
854 **53**, 1637–1647.

Figure captions

Fig. 1. Example of pyrograms from permanganate- and dichromate-oxidation resistant soil organic matter, and that from non-oxidized samples.

Fig. 2. Projection of the factor loadings of the pyrolysis products and sample scores in F1-F2 space. The corresponding pyrolysis product codes are given in Appendix A.

Fig. 3. Solid- state $^{13}C$ NMR spectra of the NaOH-extracts of untreated samples (NO-1, NO-2 and NO-3) and the NaOH-extracts of potassium permanganate and dichromate oxidized residues of S1 sample (MN-1 and CR-1) and the NaOH-extract of the potassium dichromate oxidized residues of S2 sample (CR-2).

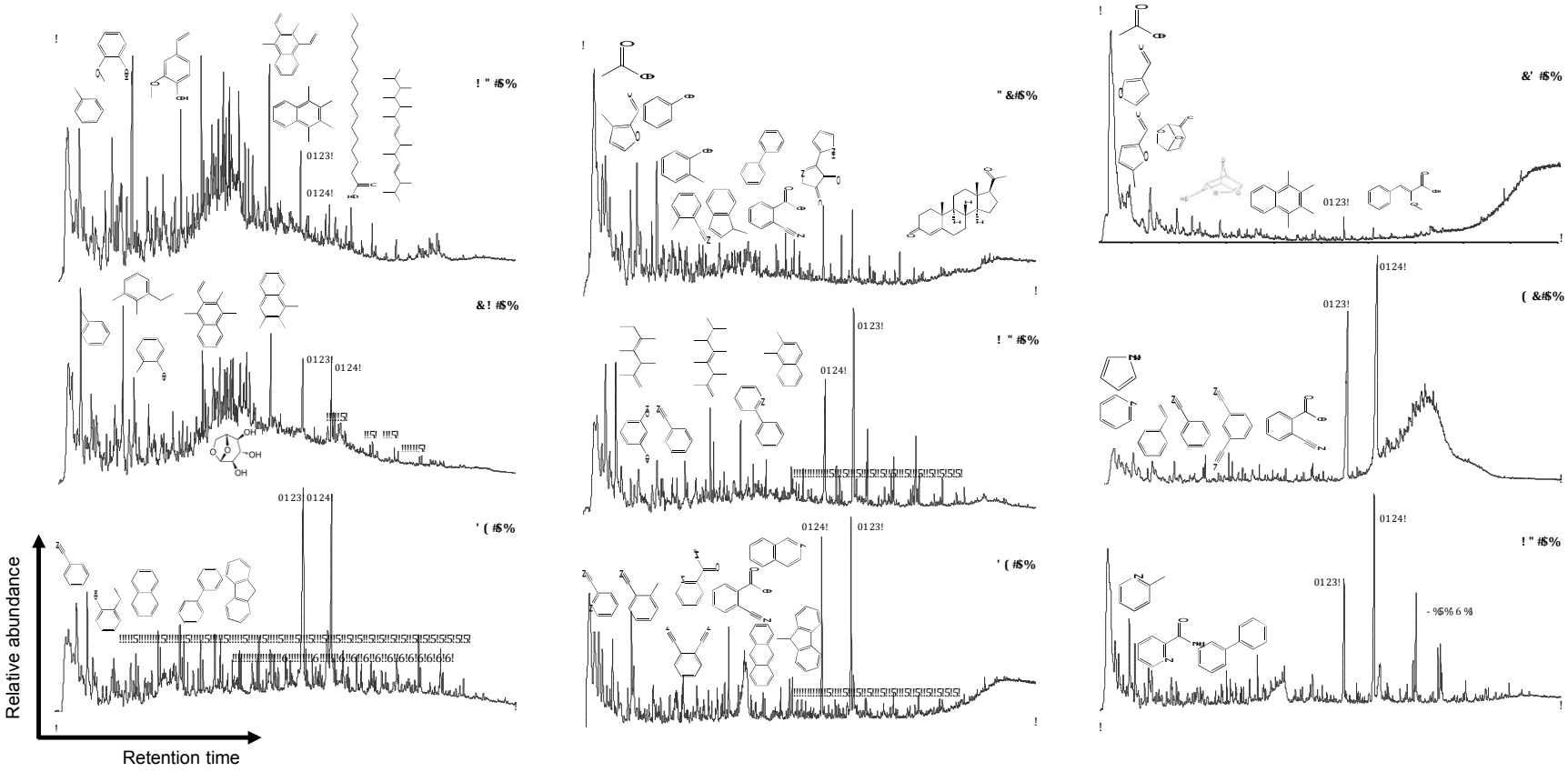
Relative abundance
Retention time
0123!
0124!

Fig. 1

NO-1: toluene, guaiacol, 4-vinyl guaiacol, $C_{4:1}$ naphthalene compound, $C_4$-naphthalene, hexadecanoic acid ($C_{16}$ *n*-fatty acid) and octadecanoic acid ($C_{18}$ *n*-fatty acid), and branched alkene. MN-1: toluene, methyl phenol, 2-ethyl 3,4-dimethyl phenol, $C_{4:1}$ naphthalene compound, levoglucosan, $C_3$-naphthalene, $C_{16}$ *n*-fatty acid and $C_{18}$ *n*-fatty acid, and series of pairs of *n*-alkanes/alkenes (*). CR-1: benzonitrile, ethyl phenol, naphthalene, biphenyl, fluorene and regular series of pairs of *n*-alkanes/alkenes (*) and *n*-fatty acids (†). NO-2: acetic acid, methyl furaldehyde, phenol, methyl phenol, methyl benzonitrile, methyl indene, biphenyl, cyanobenzoic acid, diketodipyrrole and sterol compound (preg-4-ene 3,20-dione compound). MN-2: branched alkenes, resorcinol, benzonitrile, phenyl pyridine, $C_2$ naphthalene, $C_{16}$ *n*-fatty acid and $C_{18}$ *n*-fatty acid and regular series of pairs of *n*-alkanes/alkenes (*). CR-2: pyridine carbonitrile, methyl benzonitrile, benzenedicarbodinitrile, picolinamide, anthracene, methyl fluorene, cyanobenzoic acid, isoquinoline, $C_{16}$ *n*-fatty acid and $C_{18}$ *n*-fatty acid and regular series of pairs of *n*-alkanes/alkenes (*). NO-3: acetic acid, furaldehyde, methyl furaldehyde, levoglucosenone, dianhydro-alpha, D-glucopyranose, $C_4$-naphthalene and $C_{16}$ *n*-fatty acid. MN-3: pyridine, pyrrole, styrene, benzonitrile, benzenedicarbodinitrile, cyanobenzoic acid and $C_{16}$ *n*-fatty acid and $C_{18}$ *n*-fatty acid. CR-3: methyl pyridine, picolinamide, biphenyl, $C_{16}$ *n*-fatty acid and $C_{18}$ *n*-fatty acid and a set of unidentified compounds.

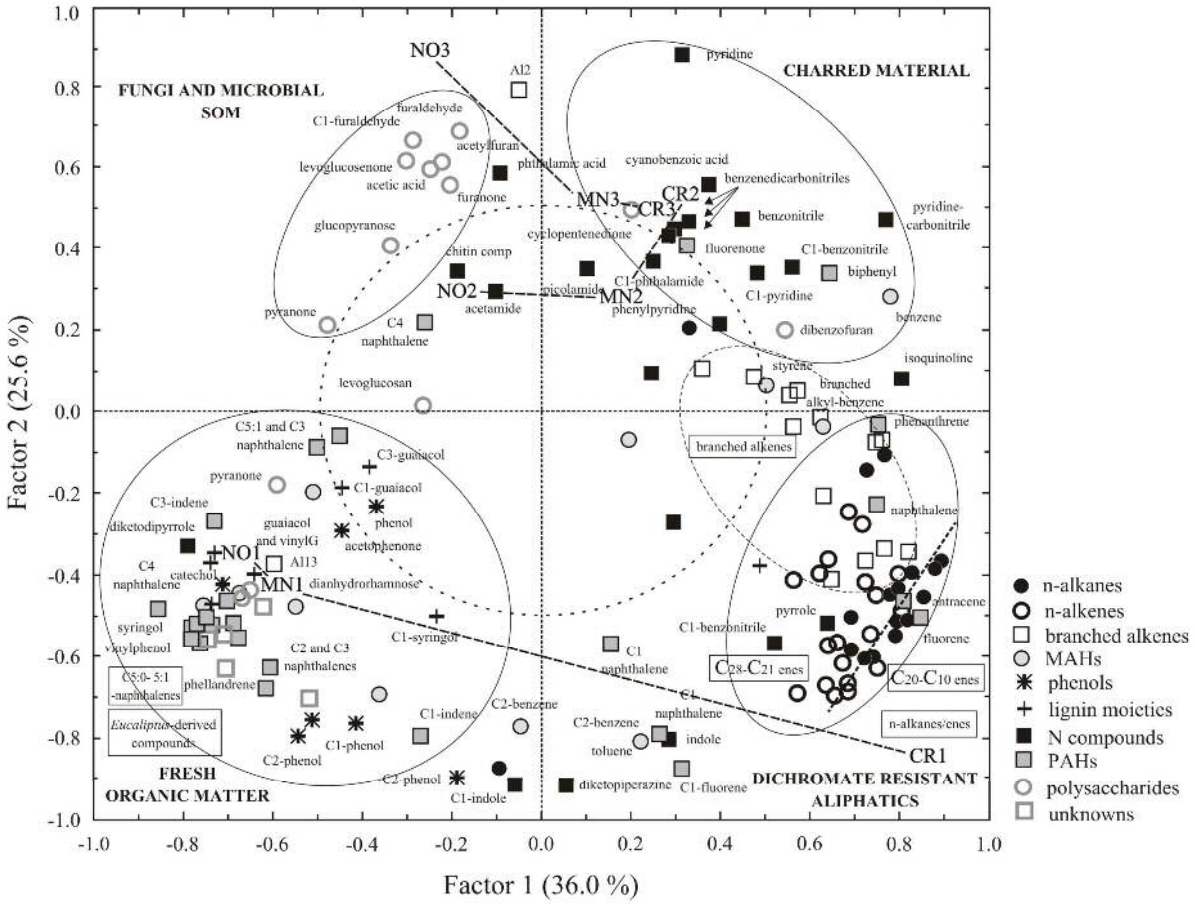


Fig.2

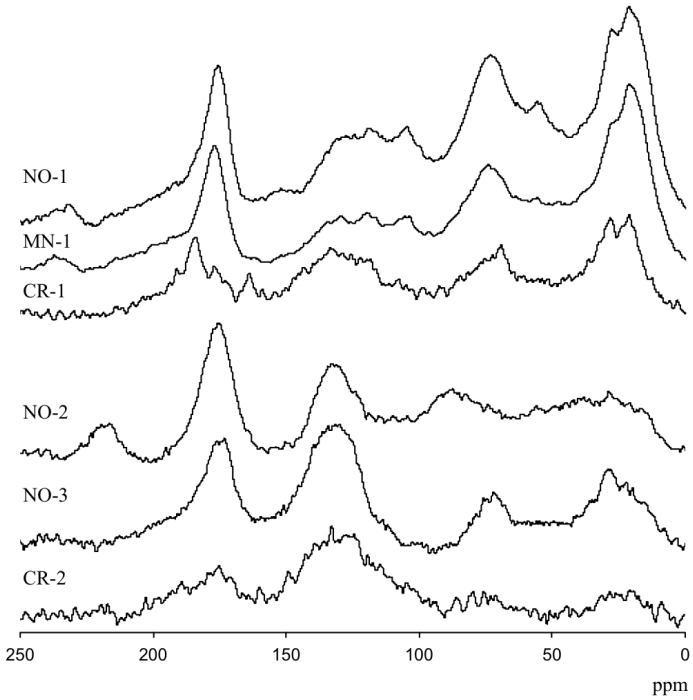


Fig.3

Table 1. General information of samples studied from soil PRD-4. $OC_{per}$ = permanganate-oxidizable organic C, $OC_{dichro}$ = dichromate-oxidizable C.

| Sample | S1 | S2 | S3 |
|---|---|---|---|
| depth | 5-10 cm | 95-100 cm | 190-195 cm |
| conventional $^{14}C$ age BP | 104.3 ± 0.4 pMC (present) | 4090 ± 30 | 9760 ± 50 |
| radiocarbon sample code | Ua-34719 | β-299230 | β-240963 |
| C [mg $g^{-1}$ soil] | 62.3 ± 0.6 | 36.7 ± 0.3 | 42.9 ± 0.4 |
| $OC_{per}$ [mg $g^{-1}$ soil] | 2.3 ± 0.1 | 1.3 ± 0.1 | 1.7 ± 0.1 |
| $OC_{dichro}$ [mg $g^{-1}$ soil] | 27.5 ± 0.6 | 12.3 ± 0.3 | 14.3 ± 0.1 |
| C/N (atomic) [-] | 15.9 | 24.4 | 23.9 |
| pH-$H_2O$ [-] | 4.6 | 5.0 | 5.2 |
| charcoal >2 mm [mg $g^{-1}$ soil] | 0.03 | 1.97 | 0.07 |

Table 2. Relative contributions of pyrolysis product groups and benzene/alkylbenzenes and PAH/alkyl-PAHs ratios of total quantified peak area (% TQPA).

| | | total n-enes | n-enes $>C_{18}$ | n-enes $C_{18}$-$C_{10}$ | total n-anes | n-anes $>C_{18}$ | n-anes $C_{18}$-$C_{10}$ | other aliph$^+$ | phs | $C_2$-ph | total Lg | total MAHs | alkyl-B | total PAHs | ITPB-PAHs | BC-PAHs | total N | BN | total Ps | well pres Ps | degr Ps | U | benz/ alkyl-benz | PAH/ alkyl-PAHs |
|---|---|---|---|---|---|---|---|---|---|---|---|---|---|---|---|---|---|---|---|---|---|---|---|---|
| NO-1 | TQPA % | **1.7** | 0.9 | 0.8 | **1.9** | 0.8 | 1.1 | 1.4 | **16.6** | 1.8 | **7.4** | **16.4** | 6.6 | **10.6** | 10.1 | 0.5 | **10.7** | 3.6 | **30.4** | 17.8 | 12.4 | 2.5 | 0.2 | 0.02 |
| | %* | | *51.4* | *48.6* | | *40.1* | *59.9* | | | | | | *40.0* | | *95.6* | *4.4* | | *33.2* | | *58.4* | *40.7* | | | |
| MN-1 | TQPA % | **1.6** | 0.5 | 1.1 | **2.0** | 0.3 | 1.7 | 4.1 | **14.1** | 1.9 | **3.0** | **30.0** | 13.4 | **12.3** | 11.4 | 1.0 | **11.7** | 4.8 | **18.4** | 10.4 | 7.7 | 2.7 | 0.2 | 0.04 |
| | %* | | *33.6* | *66.4* | | *13.4* | *86.6* | | | | | | *44.7* | | *92.2* | *7.8* | | *40.7* | | *56.6* | *41.7* | | | |
| CR-1 | TQPA % | **9.3** | 3.0 | 6.3 | **10.2** | 3.3 | 6.9 | 14.6 | **10.9** | 1.4 | **1.0** | **26.3** | 4.6 | **4.8** | 2.2 | 2.6 | **15.8** | 7.4 | **6.4** | 0.8 | 5.4 | 0.7 | 1.2 | 0.60 |
| | %* | | *32.2* | *67.8* | | *32.2* | *67.8* | | | | | | *17.5* | | *45.7* | *54.3* | | *47.0* | | *12.4* | *84.7* | | | |
| NO-2 | TQPA % | **1.8** | 0.6 | 1.2 | **1.8** | 0.6 | 1.2 | 1.7 | **13.7** | 0.8 | **1.8** | **20.4** | 4.9 | **5.7** | 4.2 | 1.5 | **20.9** | 11.9 | **31.5** | 4.0 | 27.1 | 0.7 | 0.9 | 0.21 |
| | %* | | *34.2* | *65.8* | | *34.1* | *65.9* | | | | | | *23.8* | | *73.0* | *27.0* | | *57.1* | | *12.6* | *86.3* | | | |
| MN-2 | TQPA % | **2.5** | 0.7 | 1.9 | **3.2** | 0.5 | 2.7 | 17.4 | **11.6** | 0.9 | **1.4** | **20.4** | 3.6 | **3.3** | 2.2 | 1.2 | **22.2** | 13.9 | **17.4** | 3.3 | 13.6 | 0.5 | 1.3 | 0.26 |
| | %* | | *26.0* | *74.0* | | *16.7* | *83.3* | | | | | | *17.5* | | *65.0* | *35.0* | | *62.6* | | *18.7* | *77.9* | | | |
| CR-2 | TQPA % | **4.6** | 1.6 | 3.0 | **2.5** | 0.9 | 1.5 | 7.0 | **4.8** | 0.5 | **0.8** | **16.9** | 2.0 | **3.4** | 0.9 | 2.5 | **32.2** | 23.8 | **27.6** | 15.7 | 11.5 | 0.2 | 3.9 | 1.31 |
| | %* | | *35.3* | *64.7* | | *37.7* | *62.3* | | | | | | *11.6* | | *25.3* | *74.7* | | *74.1* | | *57.0* | *41.8* | | | |
| NO-3 | TQPA % | **0.9** | 0.3 | 0.5 | **1.0** | 0.5 | 0.5 | 1.5 | **6.6** | 0.0 | **0.7** | **10.3** | 2.5 | **1.4** | 0.9 | 0.5 | **15.0** | 9.0 | **62.2** | 2.7 | 59.2 | 0.3 | 1.3 | 0.35 |
| | %* | | *36.6* | *63.4* | | *47.3* | *52.7* | | | | | | *24.0* | | *65.0* | *35.0* | | *60.2* | | *4.4* | *95.2* | | | |
| MN-3 | TQPA % | **2.7** | 0.8 | 1.9 | **2.9** | 1.2 | 1.7 | 9.2 | **7.7** | 0.0 | **1.2** | **17.5** | 4.1 | **2.4** | 1.4 | 1.0 | **38.3** | 28.9 | **17.7** | 1.1 | 16.0 | 0.4 | 0.8 | 0.34 |
| | %* | | *30.2* | *69.8* | | *42.0* | *58.0* | | | | | | *23.2* | | *57.9* | *42.1* | | *75.5* | | *6.5* | *90.7* | | | |
| CR-3 | TQPA % | **3.5** | 1.2 | 2.3 | **2.6** | 1.1 | 1.5 | 10.7 | **5.0** | 0.0 | **2.2** | **22.3** | 2.7 | **2.5** | 0.7 | 1.7 | **22.1** | 16.5 | **28.8** | 16.5 | 11.4 | 0.3 | 2.7 | 0.89 |
| | %* | | *35.0* | *65.0* | | *41.1* | *58.9* | | | | | | *11.9* | | *30.0* | *70.0* | | *74.8* | | *57.5* | *39.6* | | | |

*relative proportions within main group (*n*-alkanes/ enes, fatty acids, MAHs, PAHs, nitrogen compounds and polysaccharides). In bold the main groups.

[+]the aliphatic compound with mass 83+280 (likely associated to fresh OM) was not added because is not indicative of the charring effect.

Total *n*-enes: total *n*-alkenes; *n*-enes >$C_{18}$: long-chain *n*-alkenes (>$C_{18}$); *n*-enes $C_{18}$-$C_{10}$: short-chain *n*-alkenes ($C_{18}$-$C_{10}$); total *n*-anes: total *n*-alkanes; *n*-anes >$C_{18}$: long-chain *n*-alkanes (>$C_{18}$); *n*-anes $C_{18}$-$C_{10}$: short-chain *n*-alkanes ($C_{18}$-$C_{10}$); other aliph: other aliphatic compounds (predominantly branched alkenes); phs: phenols; total Lg: total lignin markers; total MAHs: total Monocyclic Aromatics Hydrocarbons; alkyl-B: alkyl-benzenes; total PAHs: total Polycyclic Aromatic Hydrocarbons; ITPB-PAHs: intact terpene-like plant biomass Polycyclic Aromatic Hydrocarbons; BC-PAHs: black carbon derived Polycyclic Aromatic Hydrocarbons; total N: total nitrogen compounds; BN: black carbon derived nitrogen compounds; total Ps: total polysaccharides; well pres Ps: well preserved polysaccharides; degr Ps: degraded polysaccharides; U: unidentified compounds; benz/alkyl-benz: benzene/alkyl-benzenes ratio and PAHs/alkyl-PAHs: total Polycyclic Aromatic Hydrocarbons/ alkylated Polycyclic Aromatic Hydrocarbons ratio.

Table 3. Chemical shift region distribution (relative proportions, %) obtained from solid-state $^{13}C$ NMR.

| | Alkyl C (0-45 ppm) | N-alkyl C, methoxyl C (45-60 ppm) | O-alkyl C (60-110 ppm) | C-H Aromatic C (110-140 ppm) | COR Aromatic C (140-160 ppm) | Carboxyl C, amide C (160-220 ppm) | Ketone C, aldehyde C (220-245 ppm) |
|---|---|---|---|---|---|---|---|
| NO-1 | 29 | 9 | 29 | 14 | 3 | 15 | 1 |
| MN-1 | 34 | 8 | 26 | 11 | 2 | 17 | 1 |
| CR-1 | 29 | 4 | 22 | 19 | 6 | 20 | 0 |
| NO-2 | 23 | 5 | 26 | 19 | 1 | 21 | 4 |
| CR-2 | 10 | 2 | 16 | 42 | 3 | 23 | 4 |
| NO-3 | 19 | 5 | 11 | 31 | 5 | 26 | 3 |

Appendix A. Pyrolysis product list, molecular mass ($M^+$), fragment ions used for quantification and retention times relative to guaiacol (RT).

| code | Name | $M^+$ | mass | RT/guaiacol |
|---|---|---|---|---|
| 10:1 - 28:1 | C10-28 alkene | 140 - 392 | 55+69 | 0.832 - 3.965 |
| 10:0 - 28:0 | C10-28 alkane | 142 - 394 | 57+71 | 0.857 - 3.969 |
| Al1 | aliphatic compound | n.d. | 55+70 | 0.549 |
| Al2 | alkane/anal or methylated alkanol | n.d. | 57+69+70 | 1.157 |
| Al3 | branched alkene | n.d. | 55+69 | 1.160 |
| Al4 | branched alkene | n.d. | 55+69 | 1.573 |
| Al5 | branched alkene | n.d. | 55+69 | 1.590 |
| Al6 | branched alkene | n.d. | 55+69 | 1.610 |
| Al7 | alkene | n.d. | 55+69 | 1.901 |
| Al8 | alkene | n.d. | 55+69 | 2.301 |
| Al9 | branched alkene | n.d. | 55+69 | 2.428 |
| Al10 | branched alkene | n.d. | 55+69 | 2.941 |
| Al11 | alkene | n.d. | 55+69 | 3.069 |
| Al12 | branched alkene | n.d. | 55+69 | 3.272 |
| Al13 | aliphatic compound | 83+280 | 83+280 | 3.342 |
| Al14 | branched alkene | n.d. | 55+69 | 3.565 |
| Al15 | branched alkene | n.d. | 55+69 | 3.799 |
| Ph1 | phenol | 94 | 66+94 | 0.782 |
| Ph2 | acetophenone | 120 | 77+105 | 0.937 |
| Ph3 | C1-phenol | 108 | 107+108 | 0.941 |
| Ph4 | C1-phenol | 108 | 107+108 | 0.991 |
| Ph5 | C2-phenol | 122 | 107+122 | 1.158 |
| Ph6 | C2-phenol | 122 | 107+122 | 1.202 |
| Ph7 | catechol | 110 | 110+64 | 1.348 |
| Lg1 | guaiacol | 124 | 109+124 | 1.000 |
| Lg2 | 4-methylguaiacol | 138 | 123+138 | 1.245 |
| Lg3 | 4-vinylphenol | 120 | 120+91 | 1.326 |
| Lg4 | 4-vinylguaiacol | 150 | 135+150 | 1.519 |
| Lg5 | syringol | 154 | 154+139 | 1.585 |
| Lg6 | 4-methylsyringol | 168 | 153+168 | 1.798 |
| Lg7 | C3-guaiacol | 196 | 149+164 | 1.815 |
| Lg8 | Propenoic acid, 3-(4-methoxyphenol) | 178 | 161+178 | 3.296 |
| Ar1 | benzene | 78 | 78 | 0.347 |
| Ar2 | toluene | 92 | 91+92 | 0.431 |
| Ar3 | C2-benzene ethyl benzene | 106 | 91+106 | 0.559 |
| Ar4 | C2-benzene dimethyl benzene | 106 | 91+106 | 0.574 |
| Ar5 | styrene | 104 | 78+104 | 0.605 |
| Ar6 | C2-benzene dimethyl benzene | 106 | 91+106 | 0.612 |
| Ar7 | C3-benzene | 120 | 105+120 | 0.815 |
| Ar8 | C4-benzene | 134 | 91+119 | 0.887 |
| Ar9 | C5-benzene (dimethyl-methylethyl) | 148 | 133 | 1.160 |
| Ar10 | C4:1-benzene (α-dimethylstyrene) | 132 | 132+117 | 1.026 |
| Ar11 | C7-benzene | 176 | 91+92 | 1.662 |
| Ar12 | branched alkyl-benzene | 148 | 91+119 | 1.194 |

| | | | | |
|---|---|---|---|---|
| Pa1 | C1-indene | 130 | 130+115 | 1.146 |
| Pa2 | naphthalene | 128 | 128 | 1.231 |
| Pa3 | C1-naphathalene | 142 | 141+142 | 1.491 |
| Pa4 | C1-naphathalene | 142 | 141+142 | 1.523 |
| Pa5 | biphenyl | 154 | 154 | 1.668 |
| Pa6 | C3-indene | 158 | 143+158 | 1.723 |
| Pa7 | C2-naphthalene | 156 | 141+156 | 1.772 |
| Pa8 | C3-naphthalene | 170 | 155+170 | 2.052 |
| Pa9 | C3-naphthalene | 170 | 155+170 | 2.056 |
| Pa10 | Fluorene | 166 | 165+166 | 2.090 |
| Pa11 | C3-naphthalene | 170 | 155+170 | 2.103 |
| Pa12 | C1-Fluorene | 180 | 165+180 | 2.314 |
| Pa13 | 9H-Fluoren-9-one | 180 | 152+180 | 2.353 |
| Pa14 | C4-naphthalene | 184 | 169+184 | 2.382 |
| Pa15 | phenanthrene | 178 | 178 | 2.442 |
| Pa16 | anthracene | 178 | 178 | 2.461 |
| Pa17 | C5-naphthalene | 198 | 183+198 | 2.470 |
| Pa18 | C5-naphthalene (or C2-azulene) | 198 | 183+198 | 2.643 |
| Pa19 | C5:1-naphtalene | 202 | 159+145 | 1.649 |
| Pa20 | C5-naphtalene | 204 | 147+162 | 1.739 |
| Pa21 | C5:1-naphtalene | 202 | 159+202 | 1.767 |
| Pa22 | C5-naphtalene | 204 | 91+105 | 1.801 |
| Pa23 | C5-naphtalene | 204 | 105+133 | 1.850 |
| Pa24 | C5-naphtalene | 204 | 91+105 | 1.853 |
| Pa25 | C5-naphtalene | 204 | 91+105 | 1.928 |
| Pa26 | C5-naphtalene | 204 | 91+105 | 1.974 |
| Pa27 | C5-naphtalene | 204 | 173+189 | 1.987 |
| Pa28 | C4-naphtalene | 186 | 143+171 | 2.000 |
| Pa29 | C5:1-naphtalene | 202 | 159+180 | 2.037 |
| Pa30 | C5:1-naphtalene | 202 | 146+133 | 2.143 |
| Pa31 | C5:1-naphtalene | 202 | 159+202 | 2.211 |
| N1 | pyridine | 79 | 52+79 | 0.396 |
| N2 | pyrrole | 67 | 67 | 0.402 |
| N3 | acetamide | n.d | 59 | 0.421 |
| N4 | C1-pyrrole | 81 | 80+81 | 0.501 |
| N5 | C1-pyrrole | 81 | 80+81 | 0.521 |
| N6 | C1-pyridine | 93 | 66+93 | 0.543 |
| N7 | benzonitrile | 103 | 76+103 | 0.749 |
| N8 | pyridinecarbonitrile | 104 | 104+77 | 0.887 |
| N9 | C1-benzonitrile | 117 | 90+117 | 1.011 |
| N10 | C1-benzonitrile | 117 | 90+117 | 1.067 |
| N11 | 1,3-benzenedicarbonitrile | 128 | 101+128 | 1.302 |
| N12 | picolinamide | 122 | 79+122 | 1.320 |
| N13 | 1,3-benzenedicarbonitrile | 128 | 101+128 | 1.322 |
| N14 | isoquinoline | 129 | 129 | 1.334 |
| N15 | indole | 117 | 90+117 | 1.457 |
| N16 | phthalamic acid | 104 | 104+76 | 1.457 |
| N17 | 1,3-benzenedicarbonitrile | 128 | 101+128 | 1.463 |
| N18 | C1-indole | 131 | 130+131 | 1.664 |
| N19 | C1-pthalimide | 161 | 161+76 | 1.719 |

| | | | | |
|---|---|---|---|---|
| N20 | cyanobenzoic acid | 147 | 76+147 | 1.827 |
| N21 | phenylpyridine | 155 | 154+155 | 1.833 |
| N22 | chitin-derived compound | 167 | 125+167 | 1.883 |
| N23 | diketodipyrrole | 186 | 93+186 | 2.280 |
| N24 | diketopiperazine compound | 194 | 70+194 | 2.646 |
| Ps1 | acetic acid | 60 | 60 | 0.203 |
| Ps2 | furanone compound | 84 | 54+84 | 0.434 |
| Ps3 | 3/2-furaldehyde | 96 | 95+96 | 0.483 |
| Ps4 | acetylfuran | 110 | 95+110 | 0.613 |
| Ps5 | 5-methyl-2-furaldehyde | 110 | 109+110 | 0.686 |
| Ps6 | 4-hydroxy-5,6-dihydro-(2H)-pyranone | 114 | 58+114 | 0.755 |
| Ps7 | dianhydrorhamnose | 128 | 113+128 | 0.861 |
| Ps8 | cyclopentenedione compound | 112 | 69+112 | 0.869 |
| Ps9 | levoglucosenone | 126 | 68+98 | 0.989 |
| Ps10 | 3-hydroxy-2-methyl-4H-pyran-4-one | 126 | 71+126 | 1.046 |
| Ps11 | dianhydro-α,D-glucopyranose | 144 | 57+69 | 1.263 |
| Ps12 | dibenzofuran | 168 | 168+139 | 1.953 |
| Ps13 | levoglucosan | 162 | 60+73 | 2.123 |
| U1 | alpha phellandrene | 136 | 91+93+136 | 0.827 |
| U2 | U2 (possibly methylcyclohexane) | 96 | 67+96 | 0.710 |
| U3 | U3 | 157 | 117+157 | 1.871 |
| U4 | U4 | 200 | 185+200 | 2.186 |
| U5 | U5 | 212 | 197+202 | 2.247 |
| U6 | U6 | 203 | 203 | 3.152 |